

Temperature and force characterization of an optical sag sensor for overhead line monitoring

Grzegorz Fusiek¹, Himanshi Singh^{1,2}, Pawel Niewczas¹

¹Department of Electronic and Electrical Engineering, University of Strathclyde, Glasgow, United Kingdom

²National Physical Laboratory, Teddington, Middlesex, United Kingdom

g.fusiek@strath.ac.uk

Abstract— This paper reports on the temperature and force characterization of an optical sag sensor designed for overhead line (OHL) health monitoring in electrical power networks. The proposed sensor is based on the fiber Bragg grating technology for compatibility with a suite of photonic voltage and current sensors previously developed by the authors. The sensor response was validated experimentally by subjecting it to the force load at temperatures between 20 °C and 70 °C. The characterization results demonstrated in this paper show good agreement with the simulation results (within 7% full-scale output). The outcomes of the experimental investigation show that the OHL sensor will be a suitable addition to a suite of sensors for power grid monitoring, facilitating the implementation of OHL dynamic rating and health condition monitoring functions.

Keywords— *Fiber Bragg grating, optical sag sensor, power network instrumentation, overhead power line health monitoring*

I. INTRODUCTION

Energy transmission and distribution in electrical power networks is realized by means of overhead lines (OHLs) and underground cables. Overhead lines make use of bare conductors characterized by different diameters and materials. The most common OHL conductors are made of either copper or aluminum alloys which can be additionally reinforced with steel or composite wires. They are further characterized by different number of strand wires and current carrying capacities. Current carrying capacity of the conductor vary not only with the conductor material and dimensions but also with the environmental conditions. In particular, conductor's sag is affected by its temperature which, in turn, is dependent on both the current and the environmental conditions. Therefore, monitoring of mechanical parameters of the conductors in addition to the electrical parameters of the associated power system is desirable, for example, to implement dynamic line rating.

OHL conductors are normally suspended between supporting poles or towers and hang with their middle sections below the level of the conductor ends attachment points. The vertical distance from the level of the conductor attachment to the pole and the lowest point of the hanging conductor trajectory is defined as sag. The vertical distance of the lowest point on the conductor trajectory to ground is called clearance.

Research presented in this paper was carried out within the YETIS project. YETIS is funded by Energy Catalyst, an Innovate UK program which is funded by the Foreign, Commonwealth and Development Office (FCDO). We also acknowledge the support of the Engineering and Physical Sciences Research Council and National Physical Laboratory (NPL), contributing to the associated PhD project. All data underpinning this publication are openly available from the University of Strathclyde Knowledge Base at <https://doi.org/10.15129/3e56c7e5-c1e2-421a-97df-e58b00e71c42>

The conductors are continuously in tension due to their weight and the conductor elongation is affected by thermal, elastic, and long-time creep strain. The thermal strain in the conductor varies with ambient temperature in the air and is also caused by the Joule heating due to the current in the conductor. The elastic strain varies with wind and ice loads [1]. Since the role of sag is to protect the conductor from excessive tension to avoid its damage, monitoring the level of sag is extremely important. It allows to extend the conductor lifetime and guarantee safety ensuring that sufficient clearance between the conductor and the ground is maintained. In addition, conductors are subject to wind and ice loads. Wind generates vibrations of different frequencies leading to potential damage of the conductors, for example, due to the fretting effects [2]–[4]. Therefore, monitoring conductor's structural health is also critical.

One of the techniques to increase the current carrying capacity of overhead lines in the energy transmission is the replacement of the original aluminum steel reinforced conductors with approximately the same diameter high-temperature low-sag (HTLS) conductors. HTLS conductors can withstand temperatures up to 200 °C during continuous operation without significant loss of tensile strength or increase in sag [5]. However, similarly to other overhead power lines, they would benefit from monitoring of mechanical parameters and temperature, which is more challenging to achieve at elevated temperatures.

An optical sensor solution allowing for distributed monitoring of electrical and mechanical parameters of an overhead line transmission system was previously developed by the authors. An optical sag sensor, proposed in [6], was designed to enable overhead line sag and temperature monitoring, while remaining compatible with a suite of voltage and current sensors based on the fibre Bragg grating (FBG) technology [7]–[9]. When combined with the optical voltage and current sensors, the discussed sag sensor can offer a unified single platform capability for power system dynamic rating and wide-area stability control, as well as health monitoring of overhead power lines, enabling early warnings of incipient mechanical failures.

This paper reports on the construction and characterization of an optical overhead line sag sensor previously proposed by the authors in [6]. The sag sensor combines a commercially available temperature compensated strain sensor and bespoke mechanical structures to enable installation on an overhead conductor. The sensor response to force is tested in the laboratory conditions at temperatures between 20 °C and 70 °C.

It is shown that the sensor construction ensures adequate strain transfer from the conductor and allows for measuring the conductor mechanical parameters with sufficient resolution and dynamic range.

II. SAG IN OVERHEAD POWER LINES

A. Sag and tension of the conductor

Calculations of the sag and tension in a conductor can typically be based on the catenary equation, which describes an entirely flexible rope rigidly fixed at both ends [6], [10], [11]. By using hyperbolic sine or cosine functions, the catenary equation can be defined. The equation assumes a constant weight per unit length through the conductor. A good approximation of the catenary equation can be achieved using a parabolic function. This approach assumes an invariable weight per unit horizontal length of the conductor and results in the sag value being smaller than when it is estimated with the catenary equation [6], [10].

The sag D as a function of the distance between the poles S and the actual length of the conductor L , can be expressed by the following equation [6], [10], [11]:

$$D = \sqrt{\frac{3S(L - S)}{8}} \quad (1)$$

where the difference between the conductor length L and span length S is defined as the conductor slack.

The measurements of strain in a conductor can be realized by a strain sensor installed between two anchoring clamp sets that are affixed to the conductor and separated by a certain distance. Providing there is no slippage of the clamps on the conductor surface and the strain transfer between the conductor and the sensor is ideal, the conductor sag D can be related to the measured strain by the following equation [6]:

$$D = \sqrt{\frac{3S(L_c(1 + \varepsilon) - S)}{8}} \quad (2)$$

where L_c is the initial conductor length and ε is the strain measured by the sensor equal to the change in the distance between the clamps (a relative elongation of L_c).

In (2), it is assumed that the sag sensor is attached to the conductor before it is tensioned. If the sensor is fitted after the conductor has already been tensioned, only the difference in strain $\Delta\varepsilon$, and consequently the difference in sag ΔD from the installation moment can be measured. To allow for calculations of the absolute sag and clearance to the ground, the initial horizontal tension in the conductor, as well as its initial sag and length at the conductor installation must be known [6].

III. OPTICAL SAG SENSOR

A. Conductor parameters

The sensor was designed for monitoring sag in a hard drawn copper (HDC) conductor with a cross-section area of 70 mm² and 10.5 mm diameter.

A summary of the HDC conductor parameters is listed in TABLE I.

TABLE I. CONSIDERED CONDUCTOR PARAMETERS

Parameter	Value
Material	Hard drawn copper (HDC)
Number of strands	7
Cross-section area (mm ²)	70
Diameter (mm)	10.5
weight per unit length (N/m)	5.81
Elastic modulus (GPa)	120

It is envisaged that the strain generated in the conductor at wind speeds up to 50 m/s and in the temperatures between -15 °C and 65 °C remains below 1.5 mε for an 80-m span of the conductor, as previously estimated in [6].

B. Optical strain and temperature sensor

The proposed optical OHL sag sensor utilizes a commercial strain sensor (model T220, Technica SA [12]), containing two FBGs for strain and temperature measurements. The sensor is packaged in an enclosure made of stainless steel SS316. The array of FBGs is terminated with 3 mm high temperature armored cables with strain relief buffers installed at both ends of the sensor enclosure. The packaged T220 sensor is equipped in a 0.2 mm SS304 shim allowing the sensor to be spot welded to the monitored metallic components [6].

A summary of the T220 strain and temperature sensor specifications is provided in TABLE II.

TABLE II. SPECIFICATIONS OF THE STRAIN AND TEMPERATURE SENSOR BASED ON THE MANUFACTURER'S DATA

Parameter	Value
Enclosure material	SS316
Shim material	SS304
Shim thickness (mm)	0.2
Strain range with adjustable offset (με)	±2000 or 0 ÷ 4000
Temperature range (°C)	-20 ÷ 200
Ingress protection (IP) rating	IP67
Strain accuracy including any hysteresis, nonlinearities, and the repeatability (% FS)	<0.5
Strain sensitivity (pm/με)	1.2
Temperature accuracy (°C)	<1

The sensor's operating temperatures make it suitable for the HTLS line monitoring applications.

Since the T220 strain and temperature sensor cannot be directly mounted on the overhead line conductor, suitable metallic strain transfer and attachment structures to provide measurements of sag, temperature and vibration on the

overhead line conductor were previously proposed and theoretically evaluated by the authors in [6].

C. Optical sag sensor construction

A conceptual drawing of the intended sag sensor installed on a conductor is depicted in Fig. 1. The T220 sensor is spot welded to a 2 mm thick stainless steel mounting plate secured between two sets of metal clamps and fastened to the conductor with bolts. The clamps made of SS304 are spaced by 100 mm along the conductor. An identical second plate is provided on the opposite side of the conductor to ensure symmetry of the strain response and to prevent bending of the sensor structure. The distance of the plates from the conductor is approximately 5 mm [6].

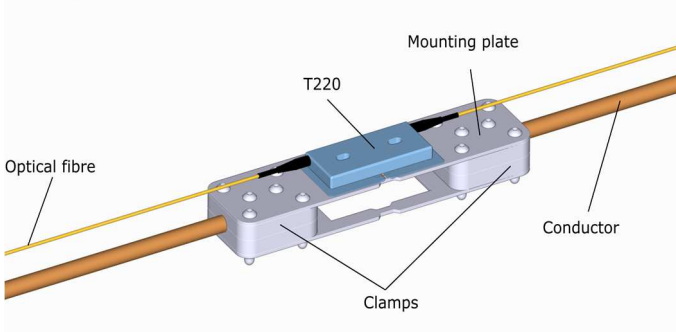


Fig. 1. Conceptual drawing of the optical sag sensor construction.

The sag sensor mounting plate is made of SS304 to match the T220 sensor shim material for welding purposes. It also aims at matching the coefficient of thermal expansion (CTE) of the conductor, so that the thermal strain in these components is similar. In addition, the selection of the sensor materials having a similar galvanic potential as the conductor material intends to minimize galvanic corrosion between these components [6], [13]. To provide additional protection of these components against moisture, and hence galvanic corrosion, the anti-corona lacquer or conductive paint can also be applied [6].

IV. SOFTWARE SIMULATIONS

Finite element analysis (FEA) was performed using the COMSOL Multiphysics® software to simulate the expected response of the sensor to strain and temperature when installed on the conductor replica.

An example of strain distribution on the surface of the rod when 1 kN load is applied at 20 °C is shown in Fig. 2.

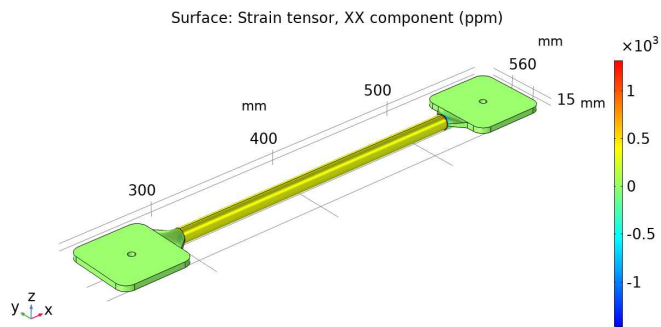


Fig. 2. Strain in the copper rod at load of 1 kN at 20°C.

In the FEA model, the sensor was attached to a copper rod and its strain response was analysed when the rod underwent an axial load from 0 kN to 5 kN at different temperatures between 20°C and 200°C. It was also assumed that the rod was fixed at one end while the axial force was applied to the other end. The length of the HDC rod was assumed to be 225 mm and the distance between the sag sensor clamps was 100 mm.

An example of the FEA results showing surface strain distribution for the modelled sag sensor construction when subjected to a force of 5 kN at a temperature of 200°C is shown in Fig. 3.

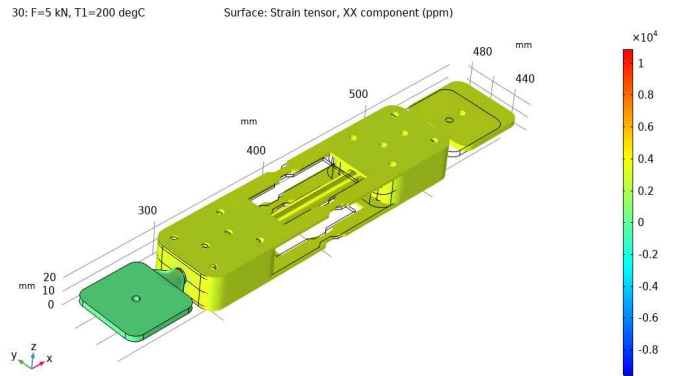


Fig. 3. Strain in the conductor at a load of 5 kN at 200°C temperature.

The relationship between the applied force and the resultant strain in the rod between the sensor clamps at various temperatures is shown Fig. 4.

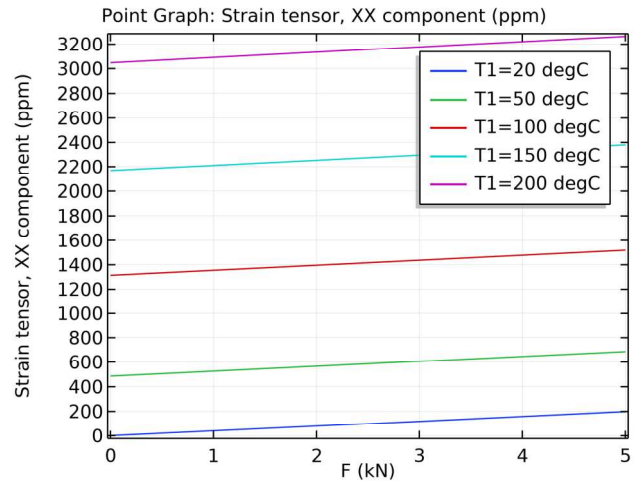


Fig. 4. Strain vs force in the conductor with a sag sensor at different temperatures.

Clearly, the mechanical strain increases with force while thermal strain increases with temperature. It should be noted that as demonstrated by the authors in [6], the strain in the rod between the clamps was 40% of the strain in the conductor outside the clamps for this type of sensor. The strain in the narrow sections of the plates was approximately 75% of the strain in the conductor outside the clamps. The benefit of this design is that the amount of strain transfer to the optical sensor

can be tailored to a particular application by modifying the width of the narrow sections of the mounting plate.

V. SAG SENSOR CONSTRUCTION

Sag sensor parts as per the design described in the previous sections were made of SS304. The sag sensor was constructed by spot-welding the strain sensor to the respected mounting plate and the plate was fixed to the conductor clamps with M5 bolts. For the strain sensor installation on the mounting plate, the fiber section with a strain measuring FBG was prestrained before spot-welding using a dedicated prestraining tool.

To assemble the sag sensor, the T220 strain sensor was first spot-welded at one end to the mounting plate with narrow sections and then the strain offset was applied to set the strain measurement range between $-1 \text{ m}\epsilon$ and $3 \text{ m}\epsilon$. The adjustment of the offset took place while the strain sensor response was monitored online using an FBG interrogator. The other end of the sensor was then spot-welded to the mounting plate. The prestressing tool was detached thereafter.

The sag sensor was then assembled and installed on the copper rod. The sensor was characterized afterwards by recording its response to force applied by a tensioning machine as described in the next section.

VI. SENSOR CHARACTERIZATION

A 10 kN electromechanical M350-10CT Testometric tensioning machine offering wide control of loading rates (speed range of 0.00001-2000 mm/min) and load measurement accuracy of $\pm 0.5\%$ down to 1/1000th of the load cell capacity was used to characterize the sensor. The machine was equipped with an oven capable of temperature cycling the sensor between 20 and 70 °C.

To verify the sag sensor response to force at temperatures between 20 and 70 °C, the sag sensor was assembled and installed on a 10.5 mm diameter copper rod being a replica of the HDC conductor. The copper rod with the sag sensor attached was placed in the machine grips as shown in Fig. 5. The reason for replacing the actual conductor with a rod was the limited space between the grips of the machine and in the oven and the difficulties in fixing the conductor in the machine grips.

The force applied in the machine was from 0 to 3 kN which was ramped up in 500 N steps over 1 min then held at a constant level for 2 min before ramping up again to the next force level. After reaching 3 kN, the force was then brought down back to 0 kN in the same fashion.

The oven temperature was increased in 10 °C steps between 20-70 °C. The oven was left for 2 h at each temperature step to achieve stable temperature before the force characterization took place. The force readings were logged by the machine's software. At the same time, the FBG center wavelength (FBG CW) shifts of the sag sensor were logged by the FBG interrogator at 1 kHz. The temperature readings were achieved by using a 4-channel PT-104 temperature logger (Pico Technology) and a PT100 platinum resistance thermometer (PRT) having the $-50 \text{ }^\circ\text{C}$ to $+250 \text{ }^\circ\text{C}$ temperature range and $\pm 0.03 \text{ }^\circ\text{C}$ accuracy.

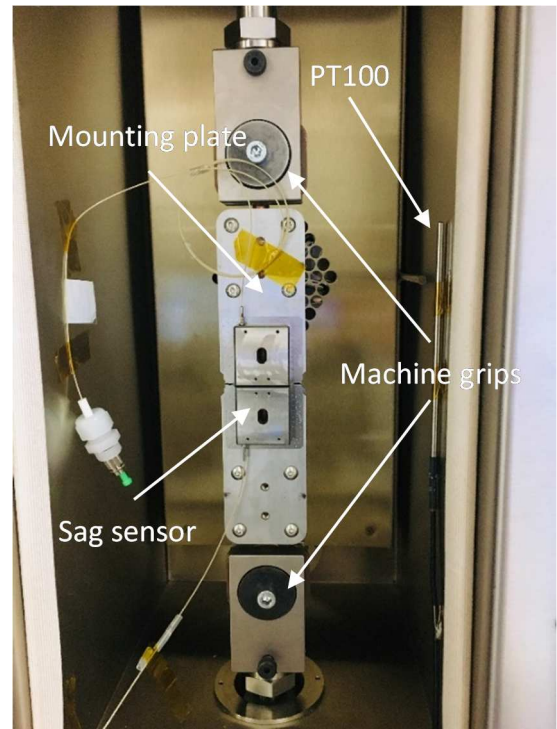


Fig. 5. Sensors under test in the Testometric tensioning machine.

The responses of the sag sensor to the applied force at temperatures between 20 °C and 70 °C are shown in Fig. 6 and Fig. 7, respectively.

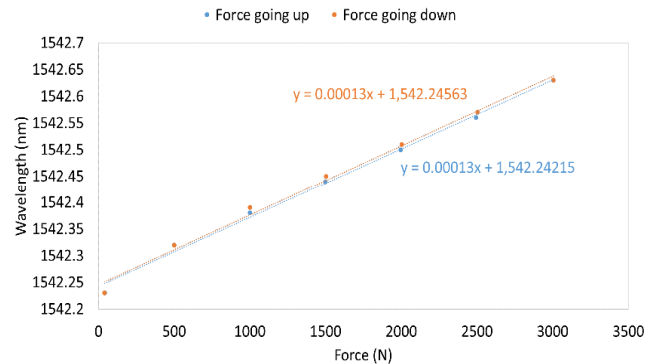


Fig. 6. Sag sensor response to force at 20 °C.

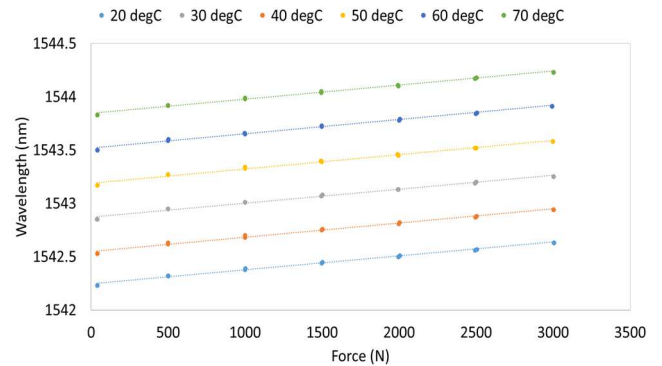


Fig. 7. Sag sensor response to force at temperatures up to 70 °C.

The response of the temperature sensor versus temperatures up to 70 °C is shown in Fig. 8.

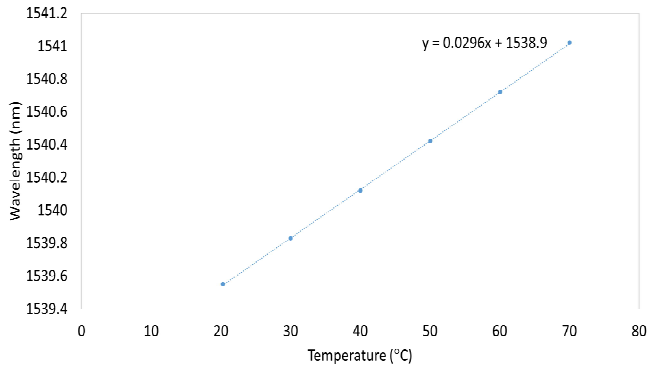


Fig. 8. Temperature sensor response to temperatures up to 70 °C.

Based on the experimental results, the wavelength sensitivity to force of the sag sensor is 0.13 ± 0.0012 nm/kN within the considered temperature range. The temperature sensor sensitivity to temperature is approximately 30 pm/°C.

Based on the T220 strain sensor calibration coefficients provided by the manufacturer, the strain detected by the sag sensor can be calculated. An example of the sag sensor strain response to the applied force at 20 °C compared to the simulation results at the same conditions is shown in Fig. 9.

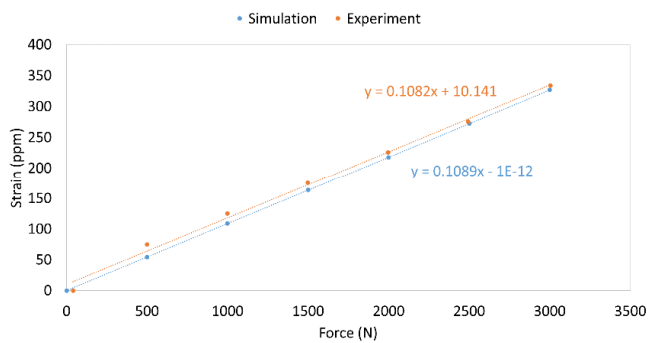


Fig. 9. Sag sensor strain response to force at 20 °C compared to the FEA results.

At a force of 3 kN, the strain detected by the sag sensor is equal to 334 ppm. From the simulations, strain in the copper rod outside the clamps of the sensor is 326 ppm at the same force. The comparison of the simulation and experimental results shows good agreement (within the 7% full-scale output error). The differences between the experimental and simulation results are attributed to the possible inaccuracy in the conductor specifications used in the FEA model.

VII. CONCLUSIONS

In this paper, the construction and characterization of a fiber Bragg grating sag sensor for overhead line health monitoring have been reported on. The sensor was integrated with metallic

components to facilitate efficient strain transfer between the conductor and the sensor. The sensor performance was experimentally evaluated and compared with the results of the finite element analysis. The experimental results showed good agreement with the theoretical results simulated in COMSOL (within 7% full-scale output error). Based on the preliminary characterization of the sag sensor it was concluded that the device should be effective for overhead line health condition monitoring and dynamic rating purposes.

Future work will concentrate on the field trials of the proposed sag sensor and its performance validation when measuring sag on the power line.

REFERENCES

- [1] L. Sjöholm, "Computational handbook for power line engineers," Stockholm, Sweden, 2017.
- [2] M. Boniardi, S. Cincera, F. D'Errico, and C. Tagliabue, "Fretting Fatigue Phenomena on an all Aluminium Alloy Conductor," in *Key Engineering Materials*, vol. 348–349, 2007, pp. 5–8.
- [3] D. Wenzheng, M. Baozhu, X. Zheng, C. Dazhi, and W. Peng, "Finite element analysis on the wire breaking rule of 1×7IWS steel wire rope," *MATEC Web Conf.*, vol. 108, pp. 7–11, 2017, doi: 10.1051/mateconf/201710801002.
- [4] CIGRE TF.WG.B2.12.3, *Technical Brochure 324: Sag-tension calculation methods for overhead lines*, no. June. 2007.
- [5] B. Subba Reddy and D. Chatterjee, "Performance evaluation of high temperature high current conductors," *IEEE Trans. Dielectr. Electr. Insul.*, vol. 23, no. 3, pp. 1570–1579, 2016, doi: 10.1109/TDEL.2016.005529.
- [6] G. Fusiek and P. Niewczas, "Design of an optical sensor with varied sensitivities for overhead line sag, temperature and vibration monitoring," in *I2MTC 2022 - 2022 IEEE International Instrumentation and Measurement Technology Conference, Proceedings*.
- [7] J. Nelson *et al.*, "Development and testing of optically-interrogated current sensors," in *2016 IEEE International Workshop on Applied Measurements for Power Systems (AMPS)*, 2016, pp. 1–5, doi: 10.1109/AMPS.2016.7602871.
- [8] G. Fusiek, J. Nelson, P. Niewczas, J. Havunen, E. P. Suomalainen, and J. Hallstrom, "Optical voltage sensor for MV networks," *Proc. IEEE Sensors*, vol. 2017-Decem, pp. 1–3, 2017, doi: 10.1109/ICSENS.2017.8234104.
- [9] G. Fusiek, P. Niewczas, N. Gordon, P. Orr, and P. Clarkson, "132 kV optical voltage sensor for wide area monitoring, protection and control applications," in *I2MTC 2020 - 2020 IEEE International Instrumentation and Measurement Technology Conference, Proceedings*, 2020.
- [10] P. Ramachandran, V. Vittal, and G. T. Heydt, "Mechanical State Estimation for Overhead Transmission Lines With Level Spans," *IEEE Trans. Power Syst.*, vol. 23, no. 3, pp. 908–915, Aug. 2008, doi: 10.1109/TPWRS.2008.926093.
- [11] M. Wydra, P. Kisala, D. Harasim, and P. Kacejko, "Overhead transmission line sag estimation using a simple optomechanical system with chirped fiber bragg gratings. part 1: Preliminary measurements," *Sensors (Switzerland)*, vol. 18, no. 1, pp. 1–14, 2018, doi: 10.3390/s18010309.
- [12] Technica SA, "T220 FBG Surface Strain Sensor." [Online]. Available: <https://technicasa.com/t220-surface-strain-sensor/>. [Accessed: 20-Jan-2023].
- [13] Alfred E. Bauer, "Stainless Steel in Waters: Galvanic Corrosion and its Prevention," *Stainl. Steel Waters Galvanic Corros. its Prev.*, p. 15.